

Published in final edited form as:

Sens Actuators B Chem. 2019 ; 301: . doi:10.1016/j.snb.2019.127076.

A photonic pH sensor based on photothermal spectroscopy

Matthew R. Hartings^{a,*}, Nathan J. Castro^{b,c}, Kathryn Gill^b, Zeeshan Ahmed^{b,*}

^aDepartment of Chemistry, American University, Washington, DC, USA

^bSensor Science Division, Physical Measurement Laboratory, National Institute of Standards and Technology, Gaithersburg, MD, USA
^cScience and Engineering,

^cInstitute for Health and Biomedical Innovation, Queensland University of Technology, Brisbane, Queensland, Australia

Abstract

Although the determination of pH is a standard laboratory measurement, new techniques capable of measuring pH are being developed to facilitate modern technological advances. Bio-industrial processing, tissue engineering, and intracellular environments impose unique measurement requirements on probes of pH. We describe a fiber optic-based platform, which measures the heat released by chromophores upon absorption of light. The optical fibers feature fiber Bragg gratings (FBG) whose Bragg peak redshifts with increasing temperature. Using anthocyanins (pH-sensitive chromophores found in many plants), we are able to correlate visible light absorption by a solution of anthocyanins to heat released and changes in FBG signal over a pH range of 2.5 to 10. We tested the ability of this platform to act as a sensor coating the fiber within a layer of crosslinked polyethylene glycol diacrylate (PEG-DA). Incorporating the anthocyanins into the PEG, we find that the signal magnitude increases over the observed signal at the same pH in solution. Our results indicate that this platform is viable for assessing pH in biological samples and point at ways to optimize performance.

Introduction

Environmental pH is a controlling factor for many chemical processes.[1–4] These processes are involved in phenomena that span a range of scientific disciplines (chemistry, materials science, biology, and environmental science) and can be felt over a range of length scales (molecular to global). Monitoring and tracking pH has been a standard laboratory practice since Sørensen's definition of pH in the early 1900's.[5] These measurements were facilitated by Beckman's development of an electronic probe for measuring hydrogen ion concentrations in the 1930's.[6] The fundamental design of Beckman's pH meter is recognized in current pH measurement techniques. The international pH standards continue to be set through electrochemical measurements of standardized solutions.

The standard pH probe is optimized to work in a research laboratory setting. Measurements are typically made on aqueous samples that are at least 10 mL in volume. For non-aqueous

*To whom correspondence should be addressed: MRH: hartings@american.edu; ZA: zeeshan.ahmed@nist.gov.

samples (from soil or biological tissue), the samples undergo homogenization and extraction into water before measurements can be made. There are commercial pH probes that are capable of making readings in volumes less than 1 μl . These measurements can even be performed *in vivo* in animal models.[7, 8] Unfortunately, the bulky nature of the associated reference electrodes and cabling do not permit long-term *in situ* measurements. Additionally, long-term measurements can be difficult to perform because of calibration issues as well as electrode fouling and clogging.

There are other types of pH probes that have been designed to monitor pH in non-traditional environments. pH-sensitive fluorophores permit sensing of intracellular pH and have a working range that typically spans 1 pH unit.[9–11] Similarly, polymeric waveguide-based sensors relying on volumetric changes due to osmotic pressure are limited to low ionic strength solution and small pH ranges of < 3 pH units.[12–16] Other polymeric waveguide sensors have used surface plasmon resonance as a means of analyzing solution pH.[17] Carbon fiber electrodes, which have been used to electrochemically monitor biological analytes *in vivo*, have also been explored as probes for measuring pH.[18] To facilitate their use, an electrode is modified with a pH-sensitive redox mediator, such as ubiquinone. The pH response, then, is dictated by the identity of the mediator used. pH-actuated materials have also been used as the platform for sensor design.[19] These materials, which change their shape with changing pH, can be generated at the micron-scale and have the potential to interface with tissue culturing constructs.

In this manuscript, we present a fiber optic-based pH measurement technique. The fiber-optic probe has several advantages over the traditional pH probe. It has a small probe size (100 μm diameter). It is free from bulky attachments. Further, it does not require any components that may fail due to clogging or fouling. These qualities may overcome some of the shortcomings, listed above, that prevent traditional probes from making accurate, long-term, *in situ* measurements over a wide range of pH values. Additionally, as fiber optics have been produced for medical applications for several decades, we expect that advances in probe technology could be readily implemented for making medically-relevant pH measurements.

Our technique uses photothermal spectroscopy and fiber Bragg grating sensors (FBGs) to monitor the environment of pH-sensitive chromophores.[20] FBGs are currently being studied for a number of sensing applications, many focusing on either temperature or strain. [21] Heat changes, resulting from light absorption by a chromophore, are measured with a fiber Bragg grating [22] (Figure 1). As the pH changes, so do the light absorption (and heat generation) properties of the chromophores. Accordingly, we find that the temperature increase upon chromophore absorption correspond to the chromophore's UV-Vis absorption spectra. Finally, we observe that chromophore incorporation within a casted hydrogel surrounding the fiber increases the observed photo-induced temperature changes. The pH range that we measure here is dictated by the chromophores that we chose for these initial experiments. For future measurements, pH measurement range and resolution will be dictated by the choice of chromophore used. A quick survey of available pH indicators can show chromophores that cover a pH range from 0 to 14. Taken together, these properties

indicate that our approach can lead to a modular pH sensor that can be modified to probe a number of currently challenging environments.

Materials and Methods

FBG were purchased from Advanced Optics Solutions[23] and their protective acrylic coating was mechanically stripped before use with a ThorLabs fiber stripping tool. Red cabbage powder (RCP) was purchased from Scientific Explorer. Litmus was purchased from Chemsavers. Low molecular weight poly(ethylene glycol)-diacrylate (PEG-DA, Mw = 570 Da) was used as a model hydrogel and crosslinked under UV with phenylbis(2,4,6-trimethylbenzoyl)phosphine oxide (BAPO). Red (638 nm \pm 5 nm, 20 mW) and green (520 nm \pm 5 nm, 20 mW) LEDs were purchased from Versalume. UV-Vis spectra were acquired on an HP 8453 UV-Vis spectrometer. 10 mmol/L buffers were made with citric acid, sodium citrate, acetic acid, sodium acetate, tris, CHES, phosphate, and MES. Buffer pH was measured with Mettler Toledo FiveGo pH probe.

The experimental setup for evaluating the temperature-increases upon illumination of pH-sensitive chromophores is outlined in Figure 1 and shown in more detail in the supporting information (Figure S1). A small glass tube (4 mm OD, 3 mm ID) is filled with a solution of RCP or litmus (a 1:10 dilution of a saturated suspension of chromophore in water with the appropriate buffer). The optical fiber is placed into the tube, which is aligned such that the excitation source overlaps the FBG sensor. Interrogation of the FBG sensor is described in detail elsewhere.[22] Briefly, the FBG sensor is probed with laser light (New Focus, TLB-6700 Velocity). The output wavelength of the laser is scanned over several nanometers. The light reflected off of the FBG is measured with a power meter (Newport). Changes in temperature induce changes in the FBG resonant wavelength. (Temperature increases result in a red shift of the FBG resonant wavelength while temperature decreases result in a blue shift.) The sample holder is enclosed within a lab-built insulating chamber generated from foam blocks. For each measurement, the FBG is interrogated for several minutes before turning on the excitation light.

For the PEG-DA studies, a custom mold was designed and 3D printed (Figure S2). A 40 mm \times 15 mm \times 0.3 mm cavity was inlaid within a 50 mm \times 20 mm \times 3 mm mold containing a notched end where the fiber was laid and perfused with the hydrogel. The casted gel was then UV-cured for 15 minutes (AnalytikJena Model CL-1000 UV Cross-linker). The coated fiber has a slightly different response to temperature (Figure S3) than the bare fiber (reference 22).

Results and Discussion

RCP was chosen as the pH-indicating chromophore for this study because of the broad, multi-color response to changes in pH. The UV-Vis spectra of RCP over all pH values studied is shown in the supporting information (Figure S4). Figure 2 highlights two of these spectra (at pH 2.5 and 10) and shows the overlap of the LED excitation sources with each of these absorption profiles.

Figure 2 also shows the temperature response of the FBG sensor under excitation from both red and green light. The graphs in Figure 2 show the averaged values for this excitation. The full, time response of the sensor during the excitation experiment is found in the supporting information (Figure S5). For these sensors, a 10 pm shift in the FBG response corresponds to a 1 °C change in temperature.[22, 24] There are several observations that can be made from the full data sets, which are important for moving this technology forward. First, some of the data sets display more noise than others. This noise is likely due to temperature fluctuations in the room (± 0.5 °C, in some cases). Second, there is some time delay (≈ 3 minutes) between the onset of excitation and the measured increase in solution temperature. These results (light-induced temperature changes matching absorption spectra and time response of the FBG probe) are similar for a system in which we use litmus instead of RCP (Figure S6).

We hypothesized that incorporating the dye directly onto the FBG sensor could decrease the response delay and, potentially, increase the observed signal due to minimization of heat dissipation in the small volume surrounding the FBG sensor. To test this result, we applied a PEG-DA coating around an FBG sensor and soaked the sensor in a saturated solution of RCP. We allowed the water to evaporate overnight, leaving the anthocyanins trapped within the PEG-DA coating. For our measurements, we aligned the excitation source with the FBG sensor and added water (Figure 3).

For measurements with both red and green light, maximum temperature changes were observed in under a minute. And, as expected, the magnitude of the signal increases for the dye-incorporated system over the system with dye in solution. In fact, the signal measured for each excitation increases by over an order of magnitude. For the green light, the measured temperature change is nearly 7 °C. Unfortunately, with long exposure times and the small volumes of water present, some water evaporation does occur and the signal changes due to evaporative cooling and mechanical effects. Additionally, some of the polymer-incorporated RCP does diffuse out of the polymer coating, altering the temperature response.

The sensor system that we present in this manuscript has several benefits over other non-traditional devices for pH detection. First, the pH discrimination range is dictated by the identity and combination of pH indicators used. In the current setup, RCP provides a mixture of anthocyanins whose color changes over a broad range of pH values. Our system can be tuned to meet the measurement requirements of specific applications by choice of pH indicator used. The narrow diameter of the fibers used (≈ 100 μm) is on the same order of magnitude as the carbon fiber micro-electrodes and microdialysis probes that are currently being used to study neurotransmitter release in the brains of living rodents.[25, 26] Finally, we expect our system to be capable of long-term measurements in biological systems as any potential surface fouling, which is detrimental to electrode-based measurement systems, will not adversely affect the measurements we perform.

The measurements presented here point a clear way forward for the development of our fiber optic-based pH measurement system. In the future, we will covalently incorporate the dye, or dyes, of interest directly into a polymer coating that surrounds the FBG sensor. This will

maximize the observed signal while minimizing any loss of dye to the measurement environment over a long measurement period. Signal-to-noise variations and sensitivity to natural temperature fluctuations can be decreased by coupling the measurement to an unmodified FBG fiber.

In this manuscript we have detailed the utility of a photonic pH sensor based on photothermal spectroscopy. Unlike volumetric based polymeric waveguide pH sensors, our device can operate in moderate ionic strength media over a broad pH range.[12] Furthermore, our measurement scheme relies on relative measurement of temperature and is hence less sensitive to small fluctuations in excitation source and dye concentration.

Supplementary Material

Refer to Web version on PubMed Central for supplementary material.

Acknowledgements

The authors would like to thank Jack Hartings for the kind donation of the RCP. MRH would like to acknowledge financial support from NIST award 70NANB18H021.

References

- (1). Doney SC; Fabry VJ; Feely RA; Kleypas JA Ocean Acidification: The Other CO₂ Problem, *Annual Review of Marine Science* 2009, 1, 169–192.
- (2). Kalbitz K; Solinger S; Park JH; Michalzik B; Matzner E Controls on the dynamics of dissolved organic matter in soils: A review, *Soil Science* 2000, 165, 277–304.
- (3). Koch M; Bowes G; Ross C; Zhang XH Climate change and ocean acidification effects on seagrasses and marine macroalgae, *Global Change Biology* 2013, 19, 103–132. [PubMed: 23504724]
- (4). Sinsabaugh RL; Lauber CL; Weintraub MN; Ahmed B; Allison SD; Crenshaw C; Contosta AR; Cusack D; Frey S; Gallo ME; Gartner TB; Hobbie SE; Holland K; Keeler BL; Powers JS; Stursova M; Takacs-Vesbach C; Waldrop MP; Wallenstein MD; Zak DR; Zeglin LH Stoichiometry of soil enzyme activity at global scale, *Ecology Letters* 2008, 11, 1252–1264. [PubMed: 18823393]
- (5). Sörensen SPL Über die Messung und die Bedeutung der Wasserstoffionenkonzentration bei Enzymatischen Prozessen, *Biochemische Zeitschrift* 1909, 21, 131–304.
- (6). Beckman AO; Fracker HE. Apparatus for testing Acidity. United States patent US2058761A 1934.
- (7). Fierro S; Seishima R; Nagano O; Saya H; Einaga Y In vivo pH monitoring using boron doped diamond microelectrode and silver needles: Application to stomach disorder diagnosis, *Scientific Reports* 2013, 3, 3257. [PubMed: 24247214]
- (8). Salkind AJ; Imran M; Mackenzie JW; Shapiro B Improving intramuscular pH needle electrode stability, *Medical instrumentation* 1981, 15, 126–127. [PubMed: 7231243]
- (9). Kermis HR; Kostov Y; Harms P; Rao G Dual Excitation Ratiometric Fluorescent pH Sensor for Noninvasive Bioprocess Monitoring: Development and Application, *Biotechnology Progress* 2002, 18, 1047–1053. [PubMed: 12363356]
- (10). Liu M; Lv Y; Jie X; Meng Z; Wang X; Huang J; Peng A; Tian Z A super-sensitive ratiometric fluorescent probe for monitoring intracellular subtle pH fluctuation, *Sensors and Actuators B: Chemical* 2018, 273, 167–175.
- (11). Tang B; Yu F; Li P; Tong L; Duan X; Xie T; Wang X A Near-Infrared Neutral pH Fluorescent Probe for Monitoring Minor pH Changes: Imaging in Living HepG2 and HL-7702 Cells, *Journal of the American Chemical Society* 2009, 131, 3016–3023. [PubMed: 19199620]

- (12). Cheng X; Bonefacino J; Guan BO; Tam HY All-polymer fiber-optic pH sensor, *Opt. Express* 2018, 26, 14610–14616. [PubMed: 29877495]
- (13). Hammarling K; Hilborn J; Nilsson H-E; Manuilskiy A Blood pH optrode based on evanescent waves and refractive index change; *SPIE BiOS; SPIE*; 2014, 8938.
- (14). Liu JN; Shahriari MR; Sigel GH Development of a porous polymer pH optrode, *Opt. Lett* 1992, 17, 1815–1817. [PubMed: 19798326]
- (15). Rendón-Romero A; Peña-Gomar M; Alvarado-Méndez E Optrodes of photonic fiber to pH sensor; *Photonics North 2012; SPIE*; 2012, 8412.
- (16). Yang XH; Wang LL Fluorescence pH probe based on microstructured polymer optical fiber, *Opt. Express* 2007, 15, 16478–16483. [PubMed: 19550938]
- (17). Zhao Y; Lei M; Liu S-X; Zhao Q Smart hydrogel-based optical fiber SPR sensor for pH measurements, *Sensors and Actuators B: Chemical* 2018, 261, 226–232.
- (18). McBeth C; Dughaiishi RA; Paterson A; Sharp D Ubiquinone modified printed carbon electrodes for cell culture pH monitoring, *Biosensors and Bioelectronics* 2018, 113, 46–51. [PubMed: 29727751]
- (19). Scarpa E; Lemma ED; Fiammengo R; Cipolla MP; Pisanello F; Rizzi F; De M Vittorio Microfabrication of pH-responsive 3D hydrogel structures via two-photon polymerization of high-molecular-weight poly(ethylene glycol) diacrylates, *Sensors and Actuators B: Chemical* 2019, 279, 418–426.
- (20). Terazima M; Hirota N; Braslavsky SE; Mandelis A; Bialkowski SE; Diebold GJ; Miller RJD; Fournier D; Palmer RA; Tam Quantities A, terminology, and symbols in photothermal and related spectroscopies (IUPAC Recommendations 2004), *Pure and Applied Chemistry* 2004, 76, 1083.
- (21). Fu D; Zhang Y.-n.; Zhang A; Han B; Wu Q; Zhao Y Novel Fiber Grating for Sensing Applications, *physica status solidi (a)* 2019, 216, 1800820.
- (22). Ahmed Z; Filla J; Guthrie W; Quintavalle J Fiber Bragg Grating Based Thermometry, *NCSL Int Meas* 2015, 10, 28–31. [PubMed: 27525049]
- (23). Certain equipment and materials are identified in this paper in order to specify the experimental procedure adequately. Such identification is not intended to imply endorsement by the National Institute of Standards and Technology, nor is it intended to imply that the materials or equipment identified are necessarily the best available.
- (24). Mihailov SJ Fiber Bragg Grating Sensors for Harsh Environments, *Sensors* 2012, 12,
- (25). Zestos AG; Kennedy RT Microdialysis Coupled with LC-MS/MS for In Vivo Neurochemical Monitoring, *Aaps Journal* 2017, 19, 1284–1293. [PubMed: 28660399]
- (26). Zestos AG Carbon Nanoelectrodes for the Electrochemical Detection of Neurotransmitters, *International Journal of Electrochemistry* 2018,

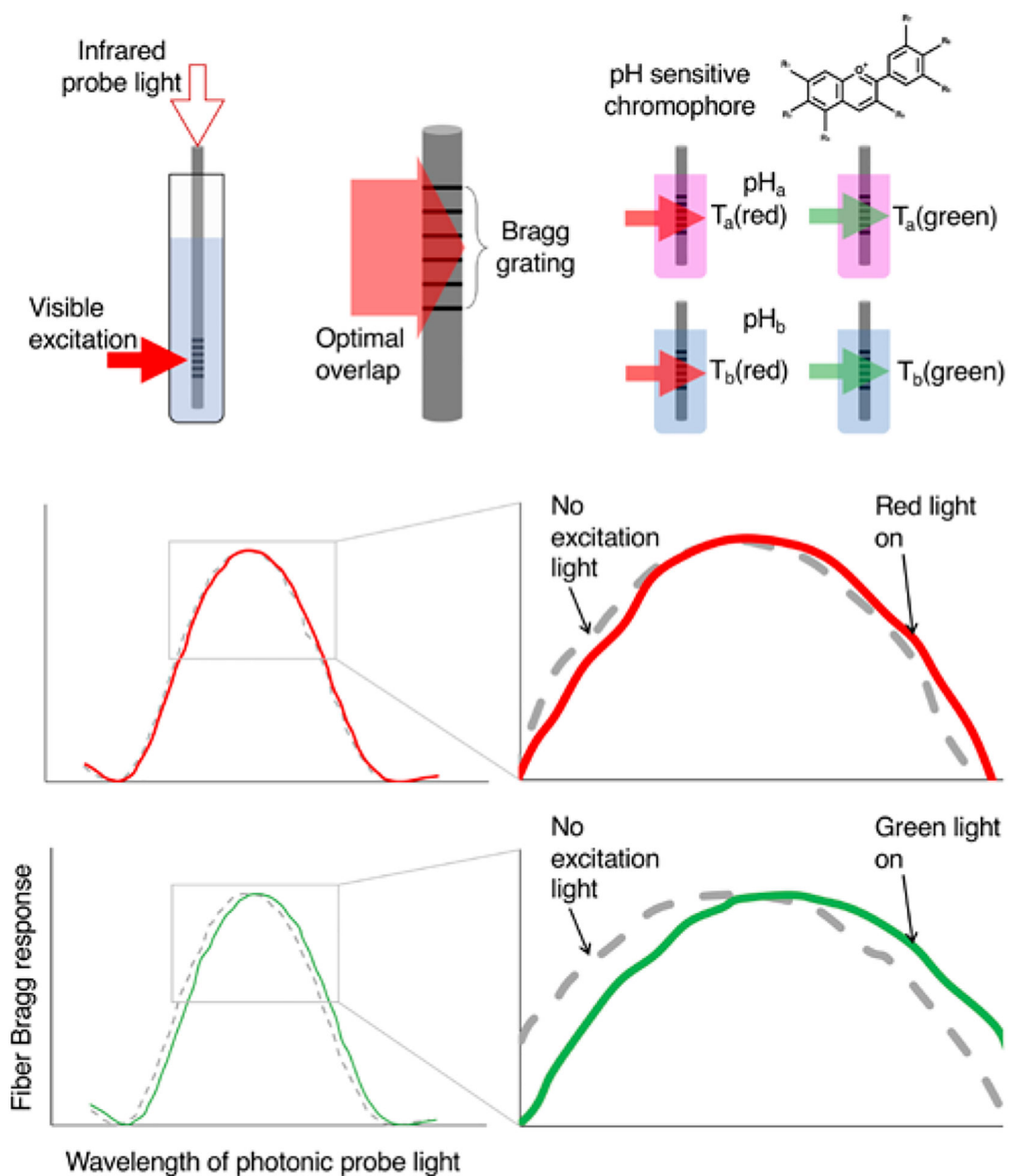


Figure 1.

Schematic outline of measurement protocol. Top left: FBG sensor placed into a chromophore solution. The sensor is interrogated with infrared light while the chromophore is excited with visible light. Top middle: To maximize the observed signal, the excitation light optimally overlaps the FBG sensor. Top right: The anthocyanin chromophores (from RCP), which take on different colors over a range of pH values, are expected to have differential temperature response based on the color of excitation light and their absorption coefficients for that light at the given pH. Middle and bottom: Examples of FBG response to increases in temperature due to photoexcitation from red (middle) and green (bottom) light.

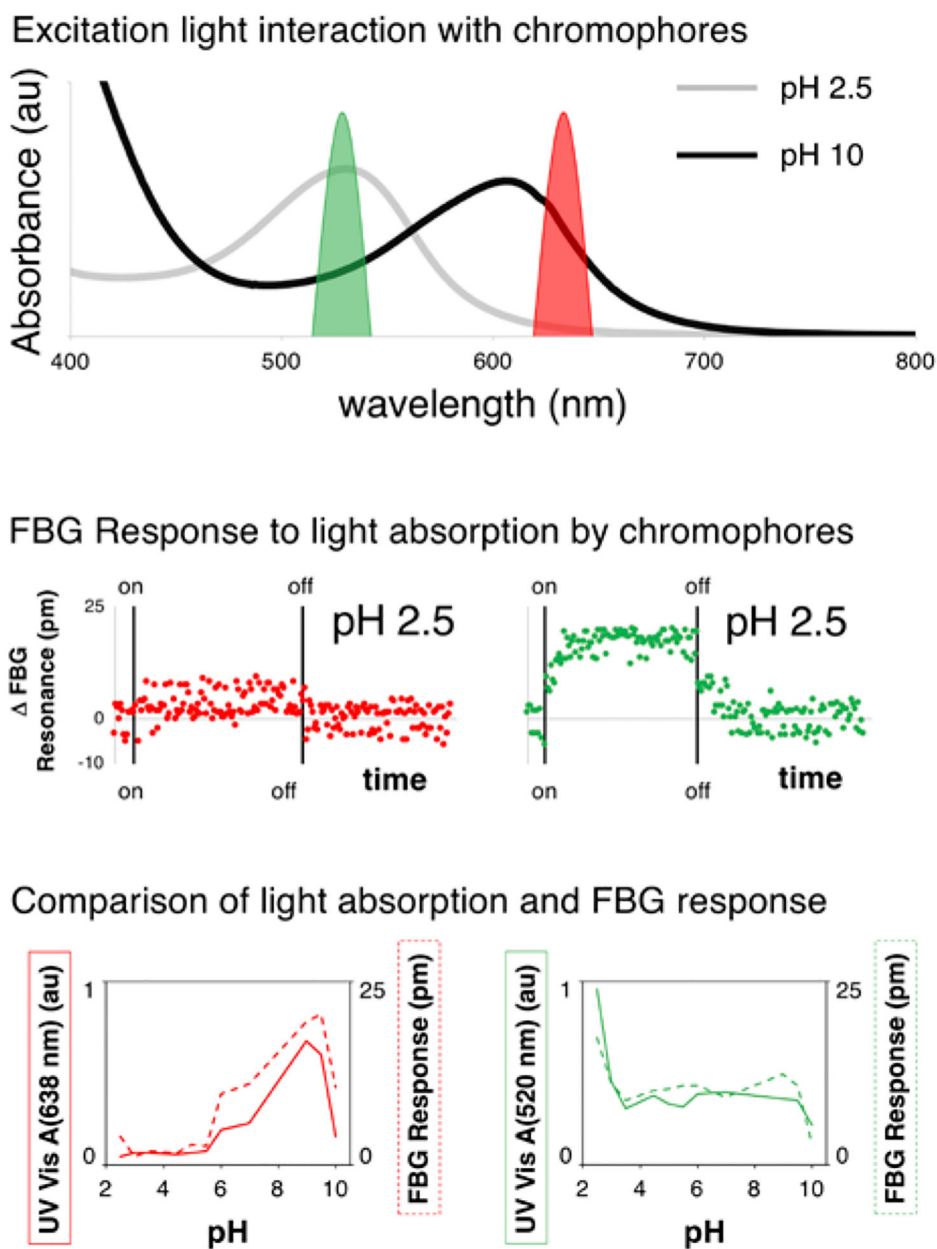
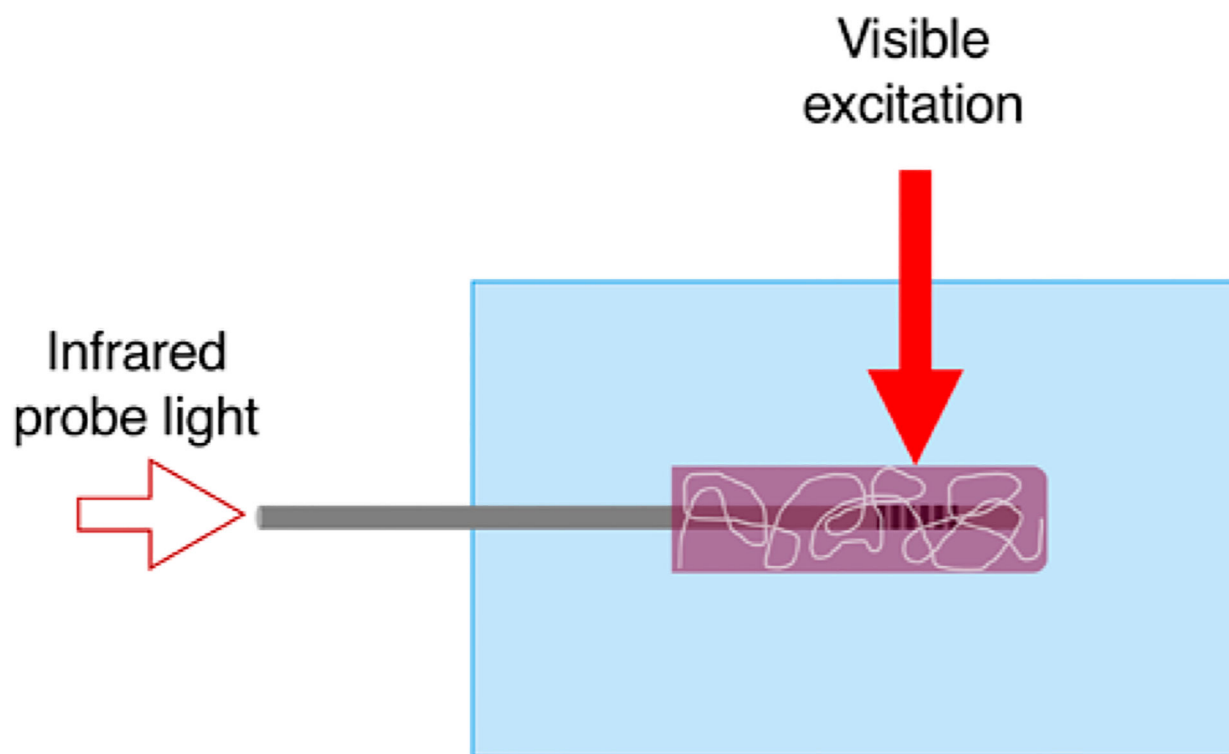


Figure 2.

Top: UV-Vis absorption spectrum of RCP at pH 2.5 (gray) and 10 (black) with the excitation profile of the LED sources (green – 520 nm and red – 638 nm). Middle: FBG response (over time) due to light absorption by chromophores at a pH of 2.5. Left – response from red light excitation. Right – response from green light excitation. Bottom left: Absorbance value at 638 nm (solid red line) and measured FBG response (dashed red line) for the RCP solution as a function of pH. Bottom right: Absorbance value at 520 nm (solid red line) and measured FBG response (dashed red line) for the RCP solution as a function of pH.



Excitation light	Average FBG Signal (nm)	max Δ FBG Response (pm)
None	1549.680	0
Red	1549.696	16
Green	1549.749	69

Figure 3. Schematic and temperature response of FBG sensor coated with RCP-containing PEG-DA. (Top) Measurement setup with RCP incorporated directly onto the FBG sensor. (Bottom) Measurement results (pH = 6). The red light (anthocyanin absorbance ≈ 0.2) elicits a lower temperature response than the green light (anthocyanin absorbance ≈ 0.4) as expected.